THE JOURNAL OF PHYSICAL CHEMISTRY B LETTERS

2006, *110,* 24277−24280
Published on Web 11/14/2006

Nanoscale Current Modulations in $Pr_{0.7}Ca_{0.3}MnO_3$ Thin Films

Hak B. Moon, Cheol H. Kim, Jai S. Ahn, and Jin H. Cho*

RCDAMP and Department of Physics, Pusan National University, Pusan 609-735, Korea

Received: September 23, 2006; In Final Form: October 25, 2006

Many theoretical and experimental efforts have been focused on the origin of the electric-pulse-induced resistance change effect. However, there are still various reports of the origin supporting either the bulk nature or the interface nature. To resolve the controversies, nanoscale electronic measurements may provide essential clues. In this work, we report microscopic electrical properties of $Pr_{0.7}Ca_{0.3}MnO_3$ thin films. The resistance of a single-crystalline grain is not homogeneous in nanometer scale. We deduce that nanoscale inhomogeneity is related to the periodic relaxation of substrate-induced strain, which is caused by the lattice mismatch between the substrate and the thin film.

1. Introduction

Manganite compounds have been of great interest for more than decade due to their technologically important colossal magnetoresistance and their subtle relation to structure. There have been many reports on manganite thin films with respect to strain. In addition, the manganite thin films show interesting columnar growth patterns on various substrates.[1] Recently, electric-pulse-induced resistance (EPIR) change was discovered from a perovskite manganese oxide $Pr_{0.7}Ca_{0.3}MnO_3$ (PCMO).[2,3] Since its discovery, it has attracted huge attention due to its high potential as a next-generation nonvolatile resistive memory device.[4−8] Many theoretical and experimental efforts have been focused on the origin of the EPIR effect. However, there are still various reports of the origin supporting either the bulk nature (the formation of current filaments)[3−5,9] or the interface nature (the tunneling through a nonpercolating domain).[10] To resolve the origin of the EPIR effect, nanoscale electronic measurements may provide essential clues. In this work, we report microscopic electrical properties of PCMO thin films. The data show that the resistance of a single-crystalline grain is not homogeneous in nanometer scale. In addition, we observe that the subtle nature of the Jahn−Teller distortion of PCMO makes it easier to adapt the strain by forming nanoscale strain relaxation. This may indicate the general tendency of structural relaxation of polycrystalline manganite compounds between grain boundaries to accommodate strains. Thus, the relaxation of strain generates defects by dislocation and/or phase separation that make current path channels.

2. Experimental Methods

The epitaxial PCMO thin films were successfully grown on $SrTiO_3$ (100) or Nb-doped $SrTiO_3$ (100) substrates by the pulsed laser deposition method. The bulk structure of PCMO used in this paper is an orthorhombic (*Pnma*) structure with lattice constants of 5.478, 7.679, and 5.426 Å.[11] A Q-switched Nd:YAG laser was used for the deposition. The target was prepared by a conventional solid-state reaction method. For a homogeneous and high-density target, stoichiometric starting material was repeatedly ground and sintered for more than 52 h at 1523, 1573, and 1593 K. For the smooth film surface, the eclipse method blocking particulates was used.[12] The energy density and repetition rate of the laser pulse were 1.2 J/cm^2 and 10 Hz, respectively. The deposition rate was estimated as ∼0.03 Å per pulse. The films with thicknesses of ∼1600 Å were grown at 1023 K under an oxygen pressure of 150 mTorr, and subsequently cooled to room temperature under 300 Torr of oxygen atmosphere. The cooling conditions were a 100 K/hr rate to get an annealed sample.

3. Results and Discussion

Nanoscale electronic data were measured using the conducting atomic force microscopy (CAFM) mode of a scanning probe microscope (Seiko Instruments, SPA400) with a gold-coated cantilever. For a high-precision CAFM measurement, an external electrometer (Keithley 6517A) and a low pass filter were used: an ∼100 fA current resolution is achieved. To study the microscopic properties, an electrical current image was obtained using a CAFM method.[13] The conducting substrate was biased with +0.1 V, and the current was measured through a conducting tip in contact mode. The measured current images of 2×2 μm^2 area are shown in Figure 1. The images show that the electrical current flows inhomogeneously in nanoscale. It also shows that current flows more on the grains themselves than through grain boundaries.

For a better understanding of local current variations in PCMO, the selected area in Figure 1 (enclosed by dashed square) is enlarged in Figure 2a. The local current variations are more clearly distinguished. From the comparison with the topographic image in Figure 2b, the current flow is smaller at grain boundaries than on the grains. In addition, there are noticeable current modulations within a single grain. For analysis, two grains were chosen, and their current profiles are depicted in Figure 2c. Current values are plotted along the lines drawn on

* Corresponding author. E-mail: jinhcho@mit.edu. Phone: 82-51-510-2968.

10.1021/jp066237k CCC: $33.50

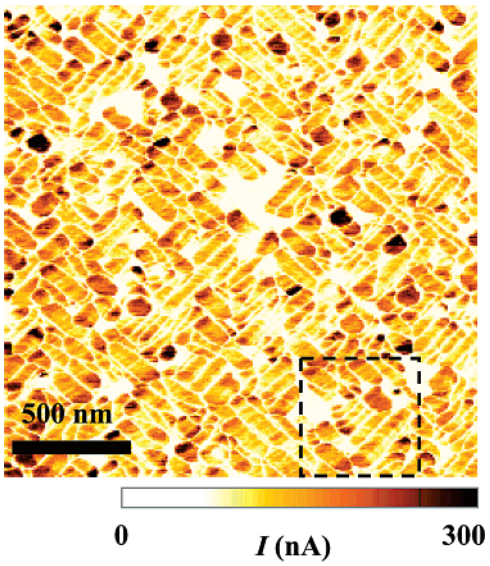

Figure 1. Current images of PCMO film obtained by CAFM. The area enclosed by the dashed square is enlarged in Figure 2a. The conducting substrate is biased with 0.1 V, and the current is scanned through a gold-coated tip in contact mode.

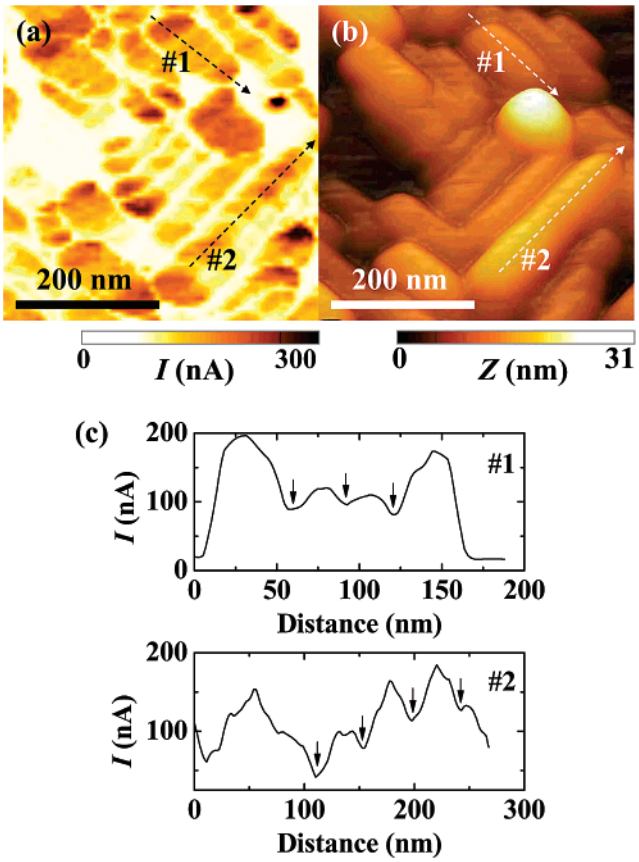

Figure 2. (a) Local current image and (b) topographic image of PCMO film. (c) Current profiles within grains #1 and #2.

top of grains #1 and #2. Distances between the periodic current valleys (indicated with arrows) are measured as 31 and 44 nm for grain #1 and grain #2, respectively. Moreover, the amplitude of intragrain current modulation is reasonably large: more than 50 nA modulation is commonly observed. To the best of our knowledge, this kind of intragrain electrical inhomogeneity is observed for the first time in PCMO. To explain our observation, we suggest two possible models: the nanoscale phase-separation

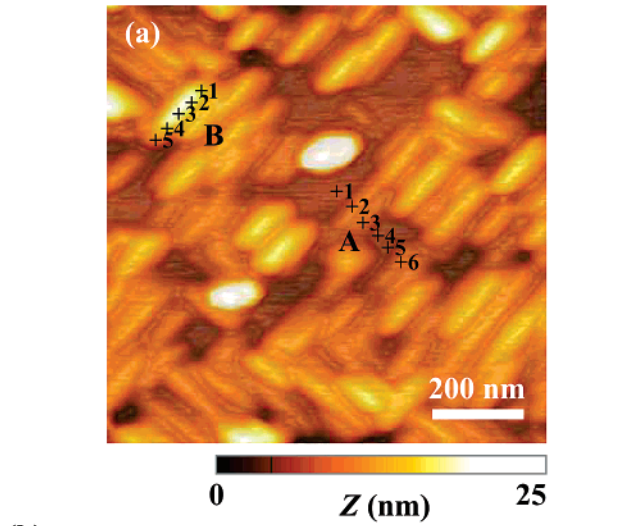

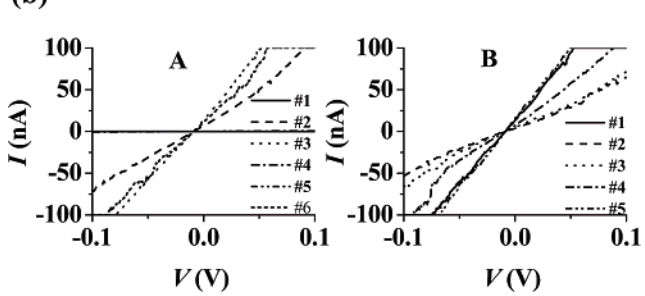

Figure 3. (a) Topographic image of region A (transverse to the grain) and B (in the grain) obtained by CAFM. (b) $I-V$ curves of regions A and B. $I-V$ data #1, #4, and #5 are overlapped in region A.

(NPS) model and the perpendicular grain-stacking (PGS) model. The NPS model describes the case in which conducting and nonconducting stripes coexist within a single grain. This NPS idea has been proposed for mixed valent manganites such as (La,Pr;Sr,Ca)MnO_3 and $Bi_{1-x}Ca_xMnO_3$, where electronic phase separation occurs in atomic scale.[14−16] Such a phase separation was also reported in PCMO at low temperatures.[17] The multilevel resistance switching behavior[4,7,18] shows the possibility of natural electrical inhomogeneity at room temperature. On the other hand, if our observation originates from the extrinsic effects such as grain boundary effect, the PGS model can be another possibility. The PGS shows the situation in which underlying grains align perpendicular to the topmost grains to relieve the strain. In this case, the tunneling current may change on the location. PCMO grains may stack on top of each other, since the thickness of the film (∼1600 Å) is much larger than the typical size of grains. However, the current image of grain #2 shows wedged-striped patterns rather than parallel ones, which cannot be understood with the simple PGS model. Therefore, the NPS model seems to be a more plausible explanation for our observations.

Current−voltage ($I-V$) curves were obtained using the CAFM mode. The electric inhomogeneity in nanoscale of the PCMO films was confirmed using $I-V$ measurement. Figure 3a shows the topography image including the $I-V$ measurement of two regions: "A" and "B". Figure 3b shows $I-V$ curves, which are transverse to the grains in region A and on top of the grain in region B. From these data, the top of the grain is more conducting than the grain boundary in the microscopic scale. More insulating $I-V$ characteristics at grain boundaries #1, #4, and #5 are overlapped and indistinguishable. I−V curves within a single grain indicate multiple current flow states between 70

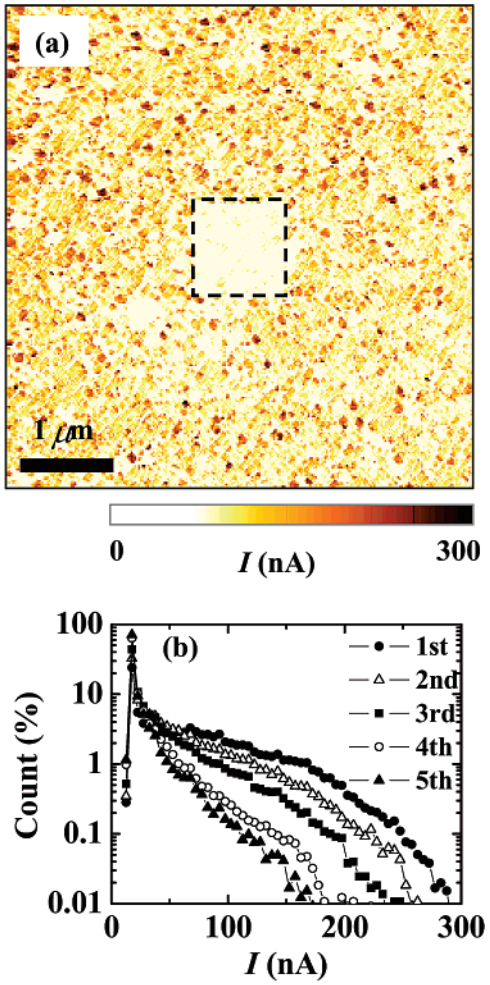

Figure 4. (a) Current image of the expanded regions: the central region is prescanned five times, and the outer region is the virgin area. (b) Change in current distributions on the central region of panel a.

nA and 200 nA. Therefore, the data show that there are many different resistance levels in a grain.

During our extensive collections of current images on various locations of PCMO films, the scan area was overlapped with the previous scan area. Unexpectedly, the current contrast of the overlapped area was clearly different from that of the fresh region. For confirmation of our observation, a new fresh region was chosen and scanned five times, consecutively. The difference between the virgin area and the five-times-scanned one is clearly visible from the current image of the expanded region (5×5 μm^2) shown in Figure 4a. The white central (1×1 μm^2) part is the five-times-scanned region. The central region is less conducting than the other region. This indicates that the sample has changed into a more insulating one with repeatedly applied bias voltage. Moreover, this electrical retention persisted more than 20 h. For a quantitative analysis of the repeating current-scan image, current values of each pixels are counted for each current scan. Figure 4b shows changes in the current distributions. Current distributions change systematically: the current distribution shifts to lower currents as scans are repeated. This observation is similar to the resistance change induced by charges traps. There are several explanations for this charging effect by carrier traps.

We suggest that one of them is that PCMO film has many current paths through crystalline defects such as dislocation, phase separation, and percolation of point defects. Since the thin films were grown at relatively low temperature, we infer that the growth is in the kinetically limited growth condition. Thus, the film growth follows local strain energy minimization to relieve the strain, as observed in the metastable columnar growth.[1] Recently, oxygen ion/vacancy motion has been suggested as an important mechanism in the EPIR effect.[19] Another report was made by Szot et al. indicating that the resistance switching effect is elucidated as the electromigration of oxygen through the network of dislocations in single-crystal $SrTiO_3$.[20] In insulating mixed-valent manganites, such an oxygen motion accompanies the Jahn−Teller distortion in MnO_6 octahedron.[21] Therefore, the Jahn−Teller stabilization energy will provide an additional energy barrier for the oxygen movement in manganites.

4. Conclusions

We present CAFM studies of resistance-changing PCMO thin films. It was found that many different resistance levels and the electrical retention behavior were observed from a CAFM study of the epitaxial PCMO film. The local CAFM data show that the intragrain current modulation originates from the electrical inhomogeneous nature such as nanoscale phase separation and/or nanoscale strain relaxation. This may indicate the general tendency of structural relaxation of polycrystalline manganite compounds between grain boundaries to accommodate strains.

Acknowledgment. This work was supported by the Korea Research Foundation Grant, KRF-2006-005-J02801. J.S.A. was partially supported by the KOSEF through CSCMR (Seoul National University). The authors appreciate Pohang Light Source and KBSI for X-ray and SEM measurements.

References and Notes

(1) Biswas, A.; Rajeswari, M.; Srivastava, R. C.; Li, Y. H.; Venkatesan, T. Greene R. L.; Millis, A. J. *Phys. Rev. B* **2000**, *61*, 9665. Van Tendeloo, G.; Lebedev O. I.; Amelincks, S. *J. Magn. Magn. Mater.* **2000**, *211*, 72. Jiang, J.; Henry, L.; Gnanasekar, K. I.; Chen C.; Meletis, E. I. *Nano Lett.* **2004**, *4*, 741.

(2) Asamitsu, A.; Tomioka, Y.; Kuwahara, H.; Tokura, Y. *Nature* **1997**, *388*, 50.

(3) Liu, S. Q.; Wu, N. J.; Ignatiev, A. *Appl. Phys. Lett.* **2000**, *76*, 2749.

(4) Odagawa, A.; Sato, H.; Inoue, I. H.; Akoh, H.; Kawasaki, M.; Tokura, Y.; Kanno, T.; Adachi, H. *Phys. Rev. B* **2004**, *70*, 224403. Odagawa, A.; Kanno, T.; Adachi, H. *J. Appl. Phys.* **2006**, *99*, 016101.

(5) Aoyama, K.; Waku, K.; Asanuma, A.; Uesu, Y.; Katsufuji, T. *Appl. Phys. Lett.* **2004**, *85*, 1208.

(6) Nian, Y. B.; Strozier, J.; Wu, N. J.; Chen, X.; Ignatiev, A. Cornell University Library arXiv database. http://arxiv.org/abs/cond-mat/0602507 (accessed 2006). Chen, X.; Strozier, J.; Wu, N. J.; Ignatiev, A.; Nian, Y. B. Cornell University arXiv Library database. http://arxiv/abs/cond-mat/0510059 (accessed 2005).

(7) Zhuang, W. W.; Pan, W.; Ulrich, B. D.; Lee, J. J.; Stecker, L.; Burmaster, A.; Evans, D. R.; Hsu, S. T.; Tajiri, M.; Shimaoka, A.; Inoue, K.; Naka, T.; Awaya, N.; Sakiyama, K.; Wang, Y.; Liu, S. Q.; Wu, N. J.; Ignatiev, A. *Tech. Dig.—IEEE Electron Devices Meet.* **2002**, 193.

(8) Baek, I. G.; Lee, M. S.; Seo, S.; Lee, M. J.; Seo, D. H.; Suh, D.-S.; Park, J. C.; Park, S. O.; Kim, H. S.; Yoo, I. K.; Chung, U.-I.; Moon, J. T. *Tech. Dig.—IEEE Electron Devices Meet.* **2004**, 587.

(9) Gibbons J. F.; Beadle, W. E. *Solid-State Electron.* **1964**, *7*, 785. Ray, A. K.; Hogarth, C. A. *Int. J. Electron.* **1990**, *69*, 97.

(10) Rozenberg, M. J.; Inoue, I. H.; Sanchez, M. J. *Phys. Rev. Lett.* **2004**, *92*, 178302. Sawa, A.; Fujii, T.; Kawasaki, M.; Tokura, Y. *Appl. Phys. Lett.* **2004**, *85*, 4073. Baikalov, A.; Wang, Y. Q.; Shen, B. Lorenz, B.; Tsui, S.; Sun, Y. Y.; Xue, Y. Y.; Chu, C. W. *Appl. Phys. Lett.* **2003**, *83*, 957. Tsui, S.; Baikalov, A.; Cmaidalka, J.; Sun, Y. Y.; Wang, Y. Q.; Xue, Y. Y.; Chu, C. W.; Chen, L.; Jacobson, A. J. *Appl. Phys. Lett.* **2004**, *85*, 317.

(11) Jirak, Z.; Krupicka, S.; Simsa, Z.; Dlouha, M.; Vratislav, S. *J. Magn. Magn. Mater.* **1985**, *53*, 153.

(12) Morita, E.; Yamamuro, K.; Tachiki, M.; Kobayashi, T. *Nucl. Instrum. Methods Phys. Res., Sect B* **1997**, *121*, 412.

(13) Cristian, I.-Z.; Mechler, A.; Carter, S. A.; Lal, R. *Adv. Mater.* **2004**, *16*, 385.

(14) Uehara, M.; Mori, S.; Chen, C. H.; Cheong, S.-W. *Nature* **1999**, *399*, 560.

(15) Renner, C.; Aeppli, G.; Kim, B.-G.; Soh, Y.-A.; Cheong, S.-W. *Nature* **2002**, *416*, 518.

(16) Capua, R. D.; Perroni, C. A.; Cataudella, V.; Granozio, F. M.; Perna, P.; Salluzzo, M.; Uccio, U. S.; Vaglio, R. Cornell University Library arXiv database. http://arxiv.org/abs/cond-mat/0605023 (accessed 2006).

(17) Martin, C.; Maignan, A.; Hervieu, M.; Raveau, B. *Phys. Rev. B* **1999**, *60*, 12191. Cox, D. E.; Radaelli, P. G.; Marezio, M.; Cheong, S.-W. *Phys. Rev. B* **1998**, *57*, 3305. Radaelli, P. G.; Ibberson, R. M.; Argyriou, D. N.; Casalta, H.; Andersen, K. H.; Cheong, S.-W.; Mitchell, J. F. *Phys. Rev. B* **2001**, *63*, 172419.

(18) Chen, X.; Wu, N. J.; Strozier, J.; Ignatiev, A. *Appl. Phys. Lett.* **2005**, *87*, 233506.

(19) Chen, X.; Wu, N. J.; Strozier, J.; Ignatiev, A. Cornell University Library arXiv database. http://arxiv.org/abs/cond-mat/0601451 (accessed 2006).

(20) Szot, K. Speier, W.; Bihlmayer, G.; Waser, R. *Nat. Mater.* **2006**, *5*, 312.

(21) Kaplan T. A.; Mahanti, S. D., Eds. *Physics of Manganites*; Kluwer Academic/Plenum: New York, 1999.